Organic Electronics 13 (2012) 599–603

Contents lists available at SciVerse ScienceDirect

Organic Electronics

journal homepage: www.elsevier.com/locate/orgel

Simple source/drain contact structure for solution-processed *n*-channel fullerene thin-film transistors

Fang-Chung Chen *, Tzung-Han Tsai, Shang-Chieh Chien

Department of Photonic and Display Institute, National Chiao Tung University, Hsinchu 30010, Taiwan

ARTICLE INFO

Article history:
Received 20 September 2011
Received in revised form 25 November 2011
Accepted 31 December 2011
Available online 17 January 2012

Keywords:
Polymer
Field effect
Transistor
Interface

ABSTRACT

This paper describes a simple approach for reducing the contact resistances at the source/drain (S/D) contacts in solution-processed *n*-channel organic thin-film transistors (OTFTs). Blending poly(ethylene glycol) (PEG) into the fullerene semiconducting layer significantly improved the device performance. The PEG molecules in the blends underwent chemical reactions with the Al atoms of the electrodes, thereby forming a better organic-metal interface. Further, the rougher surface obtained after the addition of PEG could also increase the effective contact area, thereby reducing the resistance. As a result, the electrical properties of the devices were significantly improved. Unlike conventional bilayer structures, this approach allows the ready preparation of OTFTs with a low electron injection barrier at the S/D contacts.

1. Introduction

Organic thin film transistors (OTFTs) are attracting increasing attention due to their potential applications in low-cost, flexible electronics, such as smart cards, radio frequency identification tags, and electronic paper displays [1–4]. Currently, hole mobilities higher than 1 $cm^2 V^{-1} s^{-1}$ have been widely demonstrated for *p*-channel OTFTs [3,4]. On the other hand, although high-performance *n*-channel devices have been also reported, achieving comparable performance to *p*-channel ones still remains challenging. This could be attributed to several reasons; for example, the electrons are easily trapped by the surface states, such as hydroxyl groups, at the semiconductor/dielectric interfaces, thereby decreasing the electron mobilities [5–7]. Besides, low-work-function metals, such as calcium, are usually required to reduce the electron injection barrier at the source/drain (S/D) contacts [8]. These materials are relatively difficult to handle because of their susceptibility to atmospheric moisture and oxygen. Recently, many methods for constructing effective contacts between the *n*-channel semiconductors and the S/D electrodes have been reported [9,10]. For example, Cho et al. demonstrated high-performance *n*-channel OTFTs by inserting a layer of titanium sub-oxide (TiO_x) at the electrode/semiconductor interfaces [9]. Chu et al. also used a nanoscale Cs_2CO_3 interfacial layer to reduce the S/D contact resistances [10]. However, the bilayer structures proposed in these works required one additional step to the process, which might increase the fabrication cost. In this work, we presented a simple approach for preparing high-performance *n*-channel OTFTs. We found that the device performance of solution-processable OTFTs made of [6,6]-phenyl-C_{61}-butyric acid methyl ester (PCBM) could be enhanced after the addition of poly(ethylene glycol) (PEG) into the semiconducting layer. The PEG molecules reacted with the electrode material, Al atoms, during the fabrication process of the S/D contacts; the resulting interface exhibited low contact resistances, thereby enhancing the device performance significantly [11–15].

2. Experimental

Fig. 1(a) displays the chemical structures of the materials used in this study. The OTFTs were fabricated on

* Corresponding author. Tel.: +886 3 5131484; fax: +886 3 5735601.
E-mail address: fcchen@mail.nctu.edu.tw (F.-C. Chen).

1566-1199/$ - see front matter © 2012 Elsevier B.V. All rights reserved.
doi:10.1016/j.orgel.2011.12.026

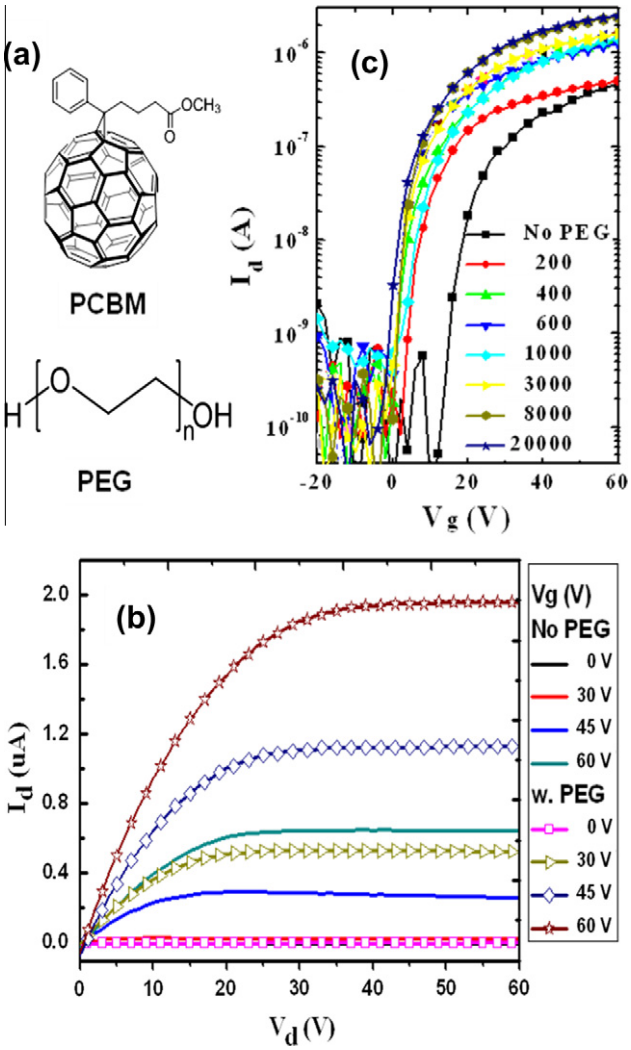

Fig. 1. (a) The chemical structures of the materials used in the work. (b) The output characteristics of the OTFTs prepared with and without PEG. The Mw of the PEG was 20,000. The optimized PCBM:PEG weight ratio was 1:0.05. (c) The transfer characteristics of the OTFTs containing PEG molecules with different molecules weights. The drain voltage (V_d) was maintained at 60 V. All the PCBM:PEG weight ratio was 1:0.05.

indium tin oxide (ITO)-coated glass substrates. The cleaned ITO substrates were then covered with a layer of 760-nm cross-linked poly(4-vinylphenol) (PVP) as the dielectric layer, which was prepared through spin-coating a solution consisting of PVP and poly(melamine-co-formaldehyde) methylated, a cross-linking agent, in propylene glycol monomethyl ether acetate [16,17]. The PVP films were firstly baked at 120 °C for 5 min and then thermally cross-linked at 200 °C for 30 min. A semiconducting layer of PCBM was subsequently deposited from a chloroform solution inside a N_2-filled glove box. The devices were then thermally annealed at 80 °C for 15 min. For the preparation of devices containing PEG, the polymer was blended into the PCBM layer at different weight ratios. Finally, 100-nm thick Al was thermally evaporated through a shadow mask to form the S/D electrodes. The channel length (L) and width (W) were 100 and 2000 μm, respectively. The current–voltage (I–V) curves were measured using the Keithley 4200 measurement system in a nitrogen environment inside a glove box. The surface morphology of the thin films was visualized using a Digital Instruments Dimension 3100 atomic force microscope (AFM).

3. Results and discussion

Fig. 1(b) shows the output characteristic of the OTFTs prepared with and without PEG. We can see that the PEG device exhibited higher output current. Apparently, the device performance was improved after the addition of PEG. To further investigate the effect of PEG, we blended PEG molecules with different molecule weights into the PCBM layer; Fig. 1(c) displays the effect of the PEG molecule weight (Mw) on the transfer characteristic of the devices. For the device made of pristine PCBM, the electron mobility, calculated from the square root of the drain current

Table 1
Characteristics of OTFTs containing PEG molecules with different molecular weights.

Molecular Weight (g/mole)	Mobility ($cm^2 V^{-1} s^{-1}$)	Threshold voltage (V)	On/off ratio
No PEG[a]	0.014	17.02	6.0×10^3
200	0.015	4.78	1.2×10^4
400	0.022	0.84	1.4×10^4
600	0.025	−0.56	1.1×10^4
1000	0.026	−0.74	1.2×10^4
3000	0.029	−0.20	1.1×10^4
8000	0.038	−0.90	2.0×10^4
20,000	0.044	−2.61	4.1×10^4

[a] Only neat PCBM was used as the semiconducting layer.

versus the gate voltage, was 0.014 $cm^2 V^{-1} s^{-1}$. The on–off ratio was only $\sim 10^3$. On the other hand, after the addition of PEG, the devices not only exhibited higher field-effect current but also showed lower threshold voltages. While the PEG Mw was 20,000, the device exhibited the highest mobility (0.044 $cm^2 V^{-1} s^{-1}$); the on–off ratio and the threshold voltage were also improved to 4.1×10^4 and −2.61 V, respectively. The device performance clearly has been improved after the use of PEG. The electrical characteristic parameters of the OTFTs were summarized in Table 1.

In order to study the mechanism responsible for the device improvement, transfer line method was further adopted to analysis the *I–V* characteristics of the devices; the results were displayed in Fig. 2 [18,19]. The device resistance was obtained from the inverse slope of the I_d–V_d curves in the linear regime. As shown in the inset of Fig. 2, the total parasitic resistance (R_p) consists two components, namely, the contact resistance (R_c) and the bulk resistance (R_b), for the top-contact device configuration. The R_p could be obtained from the $L = 0$ intersection of the linear fit of device resistances as a function of the channel length at different gate voltages. The fitting curves at different gate voltages met at an intersection point, which was the minimum effective contact resistance (R_c). The difference between R_p and R_c was equal to R_b. From the results shown in Fig. 2, we can see that the R_c was decreased significantly from 22.4 to 1.7 MΩ after the addition of PEG, suggesting that the electron injection efficiency was indeed improved. On the other hand, the R_b was relatively unchanged (~3 MΩ). Therefore, we inferred that chemical reactions between PEG molecules and Al atoms modified the nature of the S/D contacts, thereby decreasing the electron injection barrier [11–15]. More interestingly, the channel resistance (R_{ch}), which can be extracted from the slope of the fitting curves, was also decreased from 0.18 to 0.09 MΩ/μm once PEG molecules were added. Because PEG itself is insulating, we suspected that the blending of PEG also influenced the morphology of PCBM, thereby improving the charge transporting in the channel. Table 2 summarizes more detailed analysis of the device resistances for OTFTs prepared with different conditions.

To understand the origin of the device enhancement, we investigated the surface morphologies of the PCBM thin films prepared with different Mws of PEG on PVP dielectrics; the height-mode images were displayed in Fig. 3. The film containing no PEG exhibited a rather smooth surface. On the other hand, we could clearly observe phase separation on the surfaces after PEG was blended into the PCBM layer. The average diameter of the holes on top of the thin film was ~25 nm when the PEG Mw was 400 (Fig. 3(b)). In addition, we can also see that the dimension of the holes was decreased with the increasing PEG Mw, but the number of the holes was increased. These results could be explained in terms of the different diffusivities of the PEG molecules. Because PEG with a lower Mw had a higher diffusivity in the blend, more complete degree of phase separation could be achieved, thereby resulting in a larger dimension of the holes.

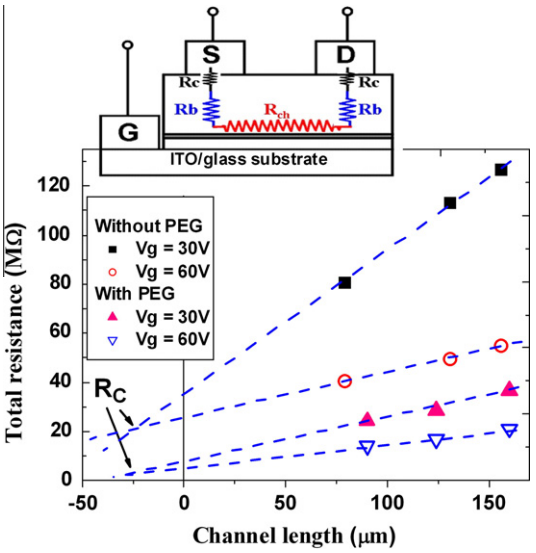

Fig. 2. The device resistance at different gate voltages as a function a channel length (*L*). The inset shows the equivalent circuit of the model. Note that R_c^S, R_c^D, R_b^S, R_b^D represent the contact resistance at the source and drain contact, and the bulk resistance at the source and drain contact, respectively.

From Fig. 3, we inferred that the PEG molecules probably did not cover the entire surface. However, the interfacial reactions should be still sufficient to decrease the charge injection barrier. Further, the AFM images apparently indicated that the thin films containing high-Mw PEG had rougher surface. Therefore, the interface should have larger effective contact area, thereby more effectively decreasing the contact resistance. As a result, the device fabricated with high-Mw PEG exhibited better device performance.

To probe possible chemical reactions at the electrode contacts, we used X-ray photoelectron spectroscopy (XPS) to study the surface of the PCBM thin films. A thin layer of Al was deposited on the thin films. Fig. 4 presents the C 1s spectra of the thin films. We can observe a main peak at a binding energy of 284.5 eV, which became boarder after PEG was blended into the thin film. We assign the shoulder at ~286.0 eV to the extra C–O bonds of PEG molecules [14]. Another peak around 289.5 eV appeared for the sample containing PEG. This additional peak was associated with the presence of higher oxidized carbon species [14]. Further, in the lower-energy regime, we could also observe some signals appeared, suggesting the forma-

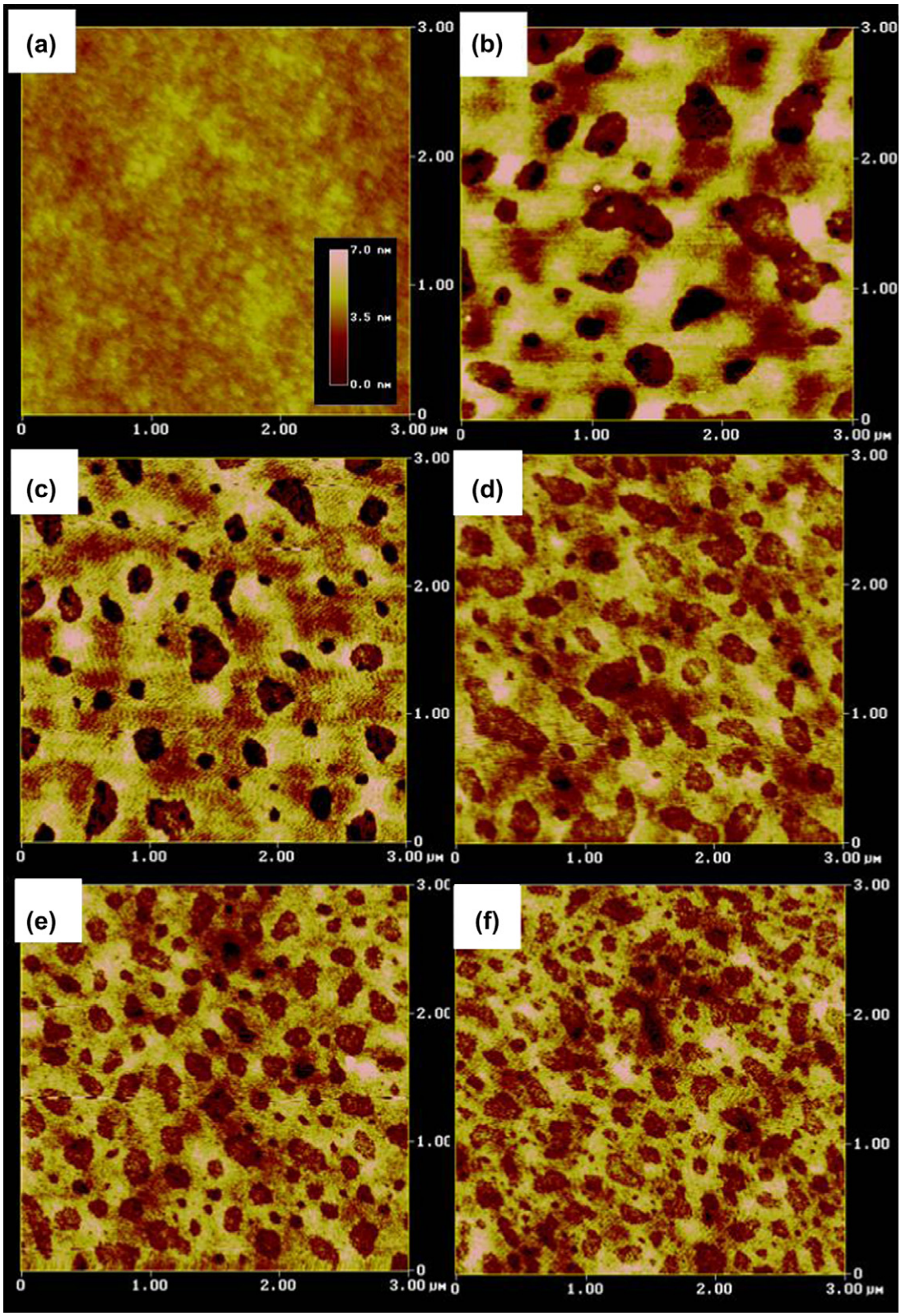

Fig. 3. (a) The height-mode AFM image of the neat PCBM film prepared on a PVP dielectric layer. (b–f) The AFM images of the PCBM blends containing PEG with different Mws. The Mw was (b) 400, (c) 1000, (d) 3000, (e) 8000 and (f) 20,000. All the image sizes are $3 \times 3\ \mu m^2$. All the PCBM:PEG weight ratio was 1:0.05.

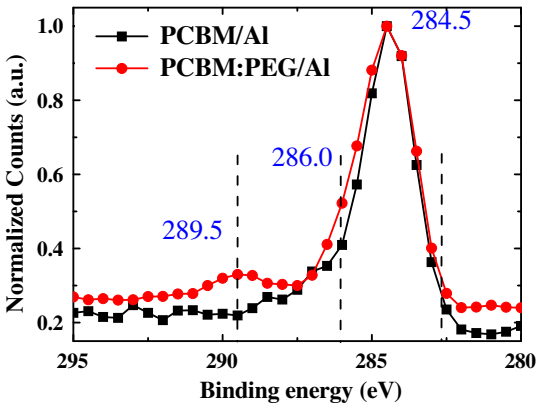

Fig. 4. The C 1s spectra of the PCBM thin films prepared with and without PEG (Mw = 20,000). A thin layer (5 nm) of Al was deposited on the thin films. The PCBM:PEG weight ratio was 1:0.05.

Table 2
Extracted resistances of the OTFTs investigated in this study following the Transfer Line-Method. The weight ratio of PCBM:PEG was kept at 1:0.05.

Molecular weight (g/mole)	Contact resistance (MΩ)	Bulk resistance (MΩ)	Parasitic resistance (MΩ)	Channel resistance (MΩ/μm)
No PEG[a]	22.4	3.4	25.8	0.18
400	6.2	2.8	9.0	0.08
1000	5.8	3.1	8.9	0.09
3000	5.2	2.4	7.6	0.07
8000	3.2	2.9	6.1	0.08
20,000	1.7	3.3	5.0	0.09

[a] Only neat PCBM was used as the semiconducting layer.

tion of carbide-like/Al complex junction [14,20]. Thus, the XPS data confirmed the chemical reactions between PEG molecules and Al atoms, which could change the nature of the interfaces and decrease the device contact resistances [20].

Finally, according to the literature [5,7], electrons are easily trapped by the hydroxyl groups on the dielectric surface. In this work, we adopted PVP as the dielectric materials. The unreacted hydroxyl groups of the cross-linked PVP might behave as electron traps, thereby leading to a lower electron mobility. To further improve the device performance, hydroxyl-free gate dielectric, such as divinyl-teamethyl-disiloxanebis(benzocyclobutene) (BCB), could be used to decrease the density of electron traps on the dielectric surface [5,21]; such studies are ongoing.

4. Conclusion

We have developed a simple approach toward high-performance solution-processed *n*-channel OTFTs. Doping PEG molecules into the PCBM layer significantly improved the device performance. The PEG molecules in the blends underwent a chemical reaction with Al atoms, thereby forming a better organic-metal contact. As a result, the electrical properties of the devices were improved. The effect of PEG Mws was also investigated; we found that the use of high-Mw PEG resulted in a rougher surface in the semiconducting layer, thereby increasing the effective contact area and decreasing the contact resistances. This approach allows the ready preparation of OTFTs with low carrier injection barrier at the S/D contacts. Moreover, unlike convention buffer layer methods, in which the electrodes are usually modified through vacuum deposition, this solution-processed approach allows printing technology to be used for device fabrication.

Acknowledgments

We thank the National Science Council of Taiwan (NSC 100-2221-E-009-082) and the Ministry of Education of Taiwan (through the ATU program) for financial support.

References

[1] Z. Bao, Adv. Mater. 12 (2000) 227.
[2] C.S. Chuang, J.A. Cheng, Y.J. Huang, H.F. Chang, F.C. Chen, H.P.D. Shieh, Appl. Phys. Lett. 93 (2008) 053305.
[3] H. Klauk, M. Halik, U. Zachieschang, G. Schmid, W. Radlik, W. Weber, J. Appl. Phys. 92 (2002) 5259.
[4] Y.Y. Lin, D.J. Gundlach, S.F. Nelson, T.N. Jackson, IEEE Electron Device Lett. 18 (1997) 606.
[5] L.L. Chua, J. Zaumseil, J.F. Chang, E.C.W. Ou, P.K.H. Ho, H. Sirringhaus, R.H. Friend, Nature 434 (2005) 194.
[6] J. Jang, J.W. Kim, N. Park, J.J. Kim, Org. Electron. 9 (2008) 481.
[7] F.C. Chen, C.H. Liao, Appl. Phys. Lett. 93 (2008) 103310.
[8] C. Waldauf, P. Schilinsky, M. Perisutti, J. Hauch, C.J. Brabec, Adv. Mater. 15 (2003) 2084.
[9] S. Cho, J.H. Seo, K. Lee, A.J. Heeger, Adv. Funct. Mater. 19 (2009) 1459.
[10] C.W. Chu, C.F. Sung, Y.Z. Lee, K. Cheng, Org. Electron. 9 (2008) 262.
[11] Y.H. Niu, H. Ma, Q. Xu, A.K.-Y. Jen, Appl. Phys. Lett. 86 (2005) 083504.
[12] T.F. Guo, F.S. Yang, Z.J. Tsai, T.C. Wen, S.N. Hsieh, Y.S. Fu, C.T. Chung, Appl. Phys. Lett. 88 (2006) 113501.
[13] X.Y. Deng, W.M. Lau, K.Y. Wong, K.H. Low, H.F. Chow, Y. Cao, Appl. Phys. Lett. 84 (2004) 3522.
[14] T.H. Lee, J. Huang, G.L. Pakhomov, T.F. Guo, T.C. Wen, Y.S. Huang, C.C. Tsou, C.T. Chung, Y.C. Lin, Y.J. Hsu, Adv. Funct. Mat. 18 (2008) 3036.
[15] F.C. Chen, S.C. Chien, J. Mater. Chem. 19 (2009) 6865.
[16] F.C. Chen, C.W. Chu, J. He, Y. Yang, J.L. Lin, Appl. Phys. Lett. 85 (2004) 3295.
[17] F.C. Chen, C.S. Chuang, Y.S. Lin, L.J. Kung, T.H. Chen, H.P.D. Shieh, Org. Electron. 7 (2006) 435.
[18] J. Zaumseil, K.W. Baldwin, J.A. Rogers, J. Appl. Phys. 93 (2003) 6117.
[19] P.V. Necliudov, M.S. Shur, D.J. Gundlach, T.N. Jackson, Solid-State Electron. 47 (2003) 259.
[20] J.Y. Jeng, M.W. Lin, Y.J. Hsu, T.C. Wen, T.F. Guo, Adv. Energy Mater. 1 (2011) 1192.
[21] S.P. Tiwari, X.H. Zhang, W.J. Potscavage Jr., B. Kippelen, J. Appl. Phys. 106 (2009) 054504.